Contiguous two-dimensional regions in the quantized Hall regime

D. A. Syphers* and P. J. Stiles
Physics Department, Brown University, Providence, Rhode Island 02912
(Received 17 June 1985)

The integer quantum Hall effect is characterized by the observance of plateaus or steps in the Hall resistance for certain regimes of density and magnetic field. These steps are centered about the midpoints between adjacent Landau levels. The value of the Hall resistance at these steps is found to be equal to h/ie^2. The two-dimensional (2D) systems that have been used previously to investigate this effect have been relatively homogeneous within their boundaries. In the quantized Hall regime the boundaries of these systems are equipotentials, with potential discontinuities occurring at the boundary with the resistive contacts where current enters or leaves the sample. The investigations discussed here explore the interaction between differently characterized macroscopic 2D regions in a given sample. These different regions are either quantized Hall regions of integer Landau-level indices or nonquantized regions. The results show that the boundary of a 2D quantized region is not necessarily an equipotential and that the interaction between different regions at the boundary between two 2D regions is determined predominantly by the values of the Hall resistance that characterize each region. As a result, the equipotential distributions for an inhomogeneous sample can be predicted. It is also shown that the current may cross the boundary between regions anywhere along its length. This leads to the solution of the "two-terminal" quantized resistance problem as potential lines are allowed to cross the boundary between a 2D quantized region and the end contacts along the entire length of the boundary.

There has been a great deal of interest generated recently in the physics of quasi-two-dimensional systems. Two startling new effects have been discovered in these systems in the last five years. The first was the discovery of the quantized Hall effect (QHE) in 1980.[1] This effect was discovered on a two-dimensional system of electrons in a Si metal-oxide-semiconductor field-effect transistor (MOSFET). The MOSFET structure is shown in Fig. 1(a). The Hall resistance of these devices was found to exhibit integer quantization, characterized by steps in the Hall resistance equal to h/ie^2, where i is an integer. This integer i corresponds to the index of the filled Landau level about which the Hall step is centered. The second new effect to be discovered was the fractional quantum Hall effect (FQHE), discovered in 1982.[2] This effect was discovered in an extremely-high-mobility layer of electrons formed in a GaAs-$Al_xGa_{1-x}As$ heterostructure. The Hall resistance in this system was found to exhibit fractional quantization, characterized by steps in the Hall resistance for certain fractional filling factors of the lower Landau levels. A representative heterostructure device is shown in Fig. 1(b).

The quantum-Hall-regime (QHR) state is marked by its nearly lossless character and by its universality; the state is observed in samples of widely differing mobility, impurity concentration, etc. Recent experiments by Fang and Stiles[3] have shown that the two-terminal resistance of a region in the QHR is equal to the Hall resistance to at least a few parts in 10^5 under usual conditions. These experiments were followed by ones combining multiple connections of a single sample to obtain rational fractions of the basic quantized resistances.[4] Together with the previously published results[5] on multiple connections of isolated samples, these experiments show that the sample is in a macroscopic lossless quantum state, where the quantized resistance is due to an interaction on a microscopic scale of the two-dimensional carriers at the interface with the source and drain contacts. Thus, in the quantum Hall regime, any two points on the perimeter will be at the same potential unless current enters or leaves the sample between those two points. This is the basis for analyzing

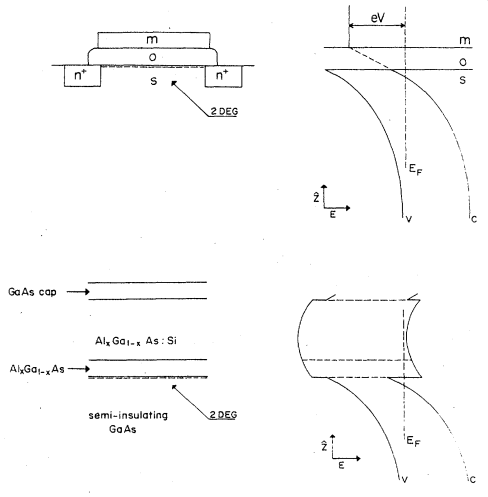

FIG. 1. MOSFET structure and GaAs-$Al_xGa_{1-x}As$ heterostructure systems with their associated band-bending diagrams. The 2D electron gas is denoted by 2DEG.

any set of multiple connections between QHR regions.

The results from these experiments raised many questions concerning the nature of the macroscopic state, and how it is affected by inhomogeneities or by the existence of other states within the quantized region. These questions are the basis for the work presented here. The primary concern addressed is the effect of macroscopic variation in density across the sample. In addition to information regarding the interaction between regions of differing density, it was hoped that this set of experiments would provide some insight into the nature of the special current-voltage profiles of samples in which the quantized Hall resistance can be observed. By the very nature of the geometric independence of the QHE, the key to this special relationship lies at the interface between a region in the QHR and other regions. In all previous experiments on the QHE, three-dimensional resistive regions were adjacent to the quantum Hall region. The experiments described here look at the interaction with other two-dimensional states.

Our experiments were performed on specially prepared devices with two distinct regions of different densities. The devices were made with two different thicknesses of oxide spanning either the length or width of a MOSFET of Hall-bar geometry. The two basic sample designs shown in Fig. 2 are the "series" regions where the boundary between the two regions is parallel with the end contacts, and the "parallel" regions where the boundary between regions is parallel with the sides of the sample. The ratio of the two oxide thicknesses is about 4:3. At a given magnetic field value, the variation of the gate voltage sweeps the carriers through the Landau levels at different rates, giving many different contiguous combinations of quantized resistance regions and nonquantized regions.

At a magnetic field of 19 T and a temperature of 1.5 K, the gate voltage was swept and the state of the sample monitored under constant-current conditions of 1 μA, source to drain. For both types of devices the monitoring included measuring two Hall voltages (one nearer the source and one nearer the drain), the potential drops along

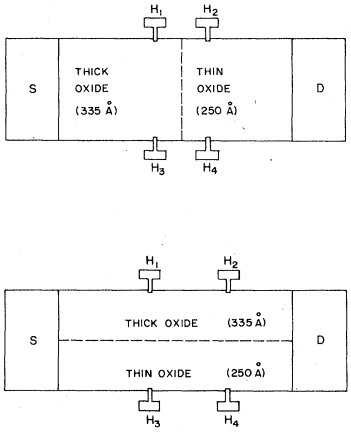

FIG. 2. Geometries for the MOSFET samples used in these experiments. The series case has the boundary between regions parallel to the end contacts, while the parallel case has it parallel to the sides of the device.

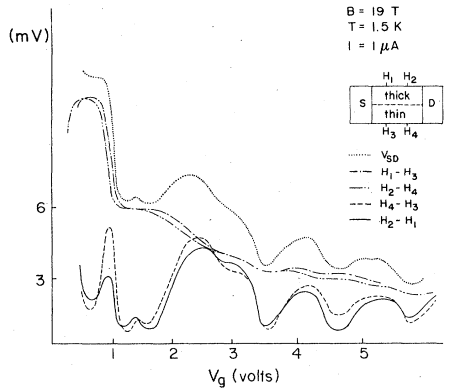

FIG. 3. Experimental results for the case of parallel contiguous regions.

both sides (proportional to ρ_{xx}) and the source-drain voltage.

The experimental results for the parallel regions are shown in Fig. 3 along with a schematic of the device. One of the first things to notice about this data is the qualitative similarity between the potential drops along either side of the sample. The drop along the side of either region does not exhibit the Landau-level oscillations expected for that region alone. These V_{xx} oscillations contain features from both regions and indicate that the interaction between the regions is dominating the state of the sample. This is most noticeable at the V_{xx} minima associated with the two $i=4$ Landau levels. The data also show a strong similarity between the two Hall voltages, as seen in Fig. 3.

The experimental results for the series regions are shown in Figs. 4 and 5 for both polarities of the magnetic field, along with the device schematic. The Hall voltages across each region exhibit the proper behavior for that region alone, with the separate Hall plateaus observed as expected. The V_{xx} potential drop across the boundary be-

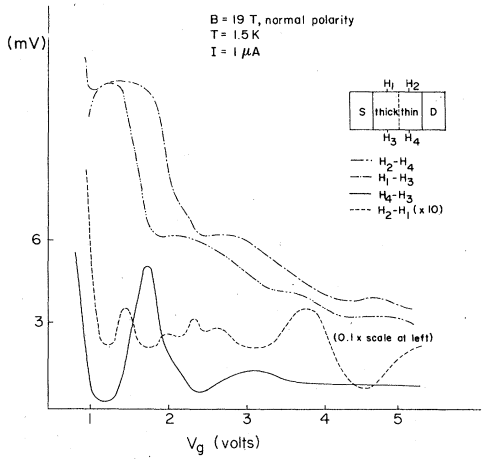

FIG. 4. Experimental results for the case of series contiguous regions with normal magnetic field polarity.

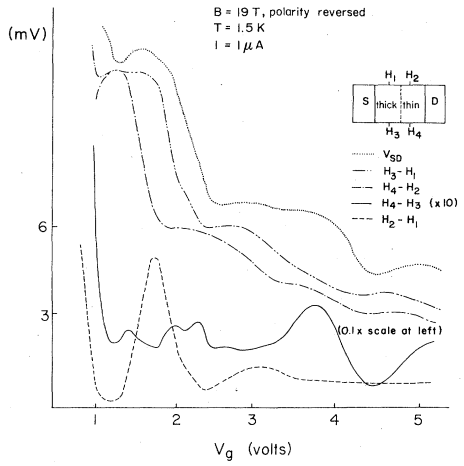

FIG. 5. Experimental results for the case of series contiguous regions with reversed magnetic field polarity.

tween regions is large on one side and much smaller on the other. This behavior of the V_{xx} potential drop across the boundary is seen to switch sides when the magnetic field is reversed. The source-drain (S-D) voltage is dominated by the region of lower density, and therefore higher overall resistance, as would be expected of series regions.

This set of data is very rich since it contains information about the interaction between two quantized regions (Q-Q'), a quantized region and a nonquantized region (Q-NQ), and two non-quantized regions (NQ-NQ') for both parallel and series configurations. The cases of interest concern the interaction with quantized regions, either Q-Q' or Q-NQ. Each of these cases will be analyzed separately for the parallel and series configurations.

It was noted from our initial work on this subject[5] that our preliminary data could be explained by two models. One model replaced the boundary between two different contiguous regions by two isolated regions with an infinite number of connections between them, and the other model held that the interaction between the two regions was determined by the relative values of ρ_{xy} for the two regions. The infinite-connection model was an extension of the model for determining the potential distribution and current paths for isolated quantized resistance regions with arbitrary interconnections.[5] This model is easily generalized to include the case of multiple connections with nonquantized regions, and is outlined in the Appendix. One of the main consequences of this model is that the current (and therefore equipotential lines) pass through the boundary between regions in a very small region at one end of the boundary for the cases of interest where at least one region is quantized. In the interactive-boundary model the current and equipotential distributions are determined by the relative values of ρ_{xy} in the contiguous regions. Hence, the current lines and equipotential lines across the boundary along its length in proportion to the relative values of ρ_{xy} of the two regions. This model covers all quantized and nonquantized cases. The experimental results are analyzed with respect to these models.

I. TWO CONTIGUOUS QUANTIZED REGIONS

A. Series regions

In this case both regions have the same current flowing through them, and we would expect the Hall voltage for each region to be determined by the quantized resistance of each region. This is observed for each region. The case of two contiguous quantized resistance regions can be seen at $V_q = 4.6$ V in Figs. 4 and 5. Here the thin oxide region is at an $i = 8$ Hall step, while the thick oxide region is at an $i = 6$ Hall step. The potential drop across the boundary between regions is equal to zero on one side of the device. The potential drop across the boundary on the other side equals the difference between the Hall voltages of the respective regions. This shows that the quantum Hall effect in each region is separately determined by the quantum state of each region. In addition, there is a very small V_{xx} potential drop across the boundary on the sides of the sample due to a small nonzero value of ρ_{xx} in each region which is observable because of the low mobility of these devices. When corrected for the nonzero value of ρ_{xx} the S-D resistance is equal to the Hall resistance of the region with the lower-Landau-level index as shown in Fig. 6. From this alone it is clear that the two regions are not acting as independent series regions.

Both models agree with these observations for series quantized regions, but give different views about the current paths and equipotential distributions within the device, as presented in the Appendix. The different distributions are shown in Figs. 12 and 13 in the Appendix. In the infinite-connection model all the current and equipotential lines must pass through an "infinitely" small region of the boundary at one side of the device. In the interactive-boundary model some of the current and equipotential lines can pass through the boundary anywhere along its length while some must pass through the boundary very near one side. This is due to the potential drop across the boundary on one side of the sample. The ratio of the current or equipotentials that can cross anywhere along the boundary to the total current or potential drop is equal to ${}^{Q}\rho_{xy}/{}^{Q'}\rho_{xy}$, where ${}^{Q}\rho_{xy}$ is the Hall resistance of the higher-Landau-index region and ${}^{Q'}\rho_{xy}$ is that of the lower-Landau-index region.

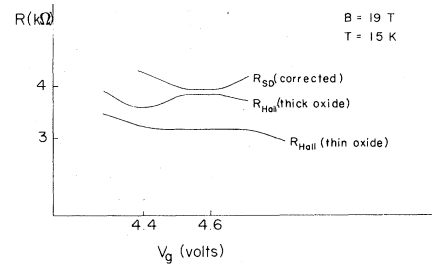

FIG. 6. Corrected value of the source-drain resistance of the series regions compared to the Hall resistance of each separate region when both regions are quantized at $V_g = 4.6$ V.

B. Parallel regions

Concurrent quantized regions are seen in Fig. 3 at $V_g = 3.6$ V. This is the same configuration as with the series regions where the thin oxide region is at an $i = 8$ Hall step and the thick oxide region is at an $i = 6$ Hall step. The Hall resistance is seen to be equal to the resistance expected at an $i = 8$ Hall step. The potential drop along both sides of the sample drops close to zero at this step. When corrected for the nonzero ρ_{xx} value of these regions, the S-D resistance is equal to the Hall resistance.

Both models agree with these results for parallel regions, and again give different views of the current paths and equipotential distributions within the device. The different distributions for this case are shown in Figs. 12 and 13 in the Appendix. In the infinite-connection model all the current or equipotential lines must pass through an "infinitely" small region of the boundary on one end of the device. In the interactive-boundary model the current and equipotential lines are allowed to pass through the boundary everywhere along its length.

It is worth noting that both models have current entering from the corner of the device and at the boundary *between* the two regions of differing density on one side of the sample. The amount of current entering at the boundary is determined by the difference between the values of ρ_{xy} of the two regions. This ensures that each region has the correct S-D voltage and Hall-current relationship (required by the QHE in each region), but raises interesting questions about the nature of current injection into any quantized regions. In the interactive-boundary model there is no high electric field at this point as there is in the corners of the device, yet current still enters there. If this model is correct, we must either accept a lossless injection of current at this point or allow the Hall angle associated with this current to be something other than 90° over some macroscopic region of the sample. Either of these options are surprising results.

Regardless of which model is correct, the existence of the current entering or leaving at the boundary gives us the ability to create new quantum resistors of new determinable values which have the same accuracy as the integer quantum Hall resistors. By stacking different quantized regions in parallel, many different resistances can be created as shown in Fig. 7. The examples shown here show how quantized resistance "sandwiches" create an effective parallel resistance. For example, a parallel combination of $i = 4,6,4$ results in an $i = 4$ current through the whole device plus an "extra" current flowing only through the $i = 6$ region. This results in an effective Hall resistance of an $i = 4$ resistor in parallel with a resistance equal to the difference between an $i = 4$ and an $i = 6$ quantum resistance.

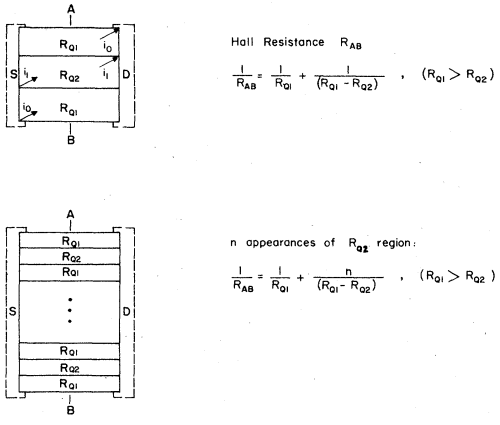

FIG. 7. The resistances and structure of quantum Hall resistor "sandwiches." The arrows in the structure at the top show the current entrance and exit paths at the corners of each quantized region.

II. A QUANTIZED AND A NONQUANTIZED REGION

A. Series regions

The two best examples of the effects of a quantized and a nonquantized region in series are the $i = 4$ Hall steps centered about $V_g = 2.0$ and 2.6 V as shown in Figs. 4 and 5. On one side of the sample the potential drop across the boundary is equal to the difference between the Hall voltages, just as in the case of two quantized regions. The other side of the sample has no potential drop across the boundary, but a small V_{xx} potential drop is seen between the probes due to the nonzero value of ρ_{xx} of the nonquantized region.

Here the two models for this contiguous system give very different predictions for the potential drop between one of these pairs of probes near the boundary. They both predict the same potential drop across the boundary on the side where the drop is not equal to zero, but give different predictions for the V_{xx} potential drop between probes on the side where there is no drop across the boundary. For both models the potential drop is due to the nonzero value of ρ_{xx} in the nonquantized region. The different predictions arise from the different current paths required by the two models as shown in the Appendix. Unlike the interactive-boundary model, the infinite-connection model requires *all* the current to pass through a small region near one side of the boundary. The resulting approximate potential distributions are shown in Fig. 8 for both models and both cases of thin and thick quantized oxides. These distributions are drawn for the case where the value of ρ_{xy} for the two regions is similar, as is the case for two $i = 4$ examples shown in Figs. 4 and 5.

When the thin oxide region is nonquantized the infinite-connection model states that V_x should be about a factor of 2 greater than when the thick oxide region is nonquantized for the same value of ρ_{xx} of the nonquantized regions. This difference is due to the different "entrance" and "exit" points of the current in the nonquantized regions as shown in Fig. 8. The value of V_x for these two situations is predicted to be about the same by the interactive-boundary model since most of the current is allowed to pass through the boundary anywhere along its length. In reality, the ratio of ρ_{xx} for a region characterized by $i < 4$ to a region characterized by $i > 4$ is of the order of 7:5 for these devices. This would mean that V_x should be about a factor of 3 greater when the thin oxide region is quantized in the infinite-connection model, and

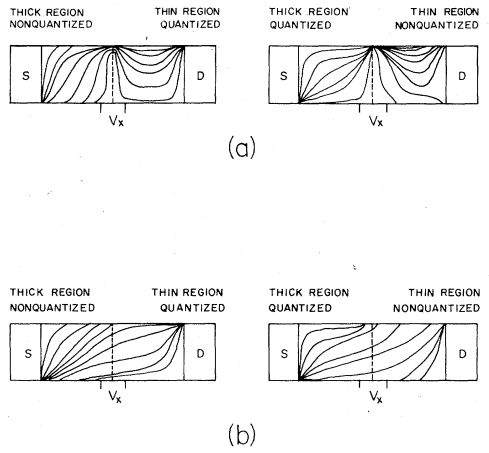

FIG. 8. Approximate distribution of equipotentials in series regions are predicted by (a) the infinite-connection model and (b) the interactive-boundary model. In (a) the requirement on current flow at the boundary results in very different equipotential distributions in the nonquantized region for the two cases shown due to the different "entrance and exit" points of the current at the boundary.

about 7:5 in the interactive-boundary model. The experimental plot of V_x versus V_g (and corrected for the actual position of the boundary relative to the potential probes) is shown in Fig. 9. The ratio of the peak V_x values for the respective $i=4$ quantized regions is seen to be about 8:5. This is well below the factor of 3 required by the infinite-connection model and is very close to the ratio of 7:5 required by the interactive-boundary model. In addition, Fig. 9 shows the experimental value of the source-drain resistance (R_{SD}) along with those values of R_{SD} calculated from the observed V_x potential drop. It shows that R_{SD} can be closely calculated from the interactive-boundary model, but is overestimated by the infinite-interconnection model.

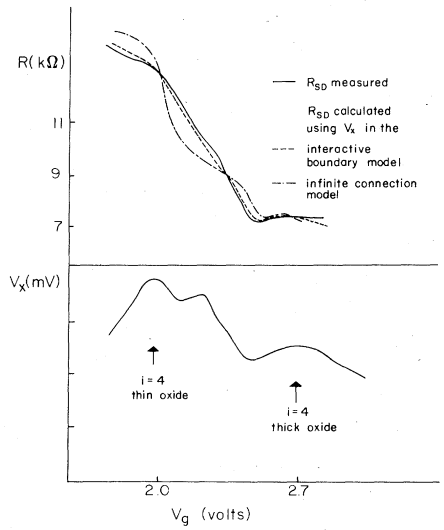

FIG. 9. The V_x potential drop and source-drain resistance as a function of gate voltage for the series regions. The positions of the respective $i=4$ Landau levels are indicated by the arrows.

B. Regions in parallel

Three important examples of a nonquantized region in parallel with a quantized region are shown in Fig. 3 at $V_g=1.25$, 1.6, and 4.8 V. The first two examples correspond to the $i=4$ Hall steps of the thin and thick oxide regions, respectively. The last example corresponds to the $i=8$ Hall step of the thick oxide region. For all these examples the potential drop along the side of the nonquantized region is larger than the drop on the side of the quantized region. The example at $V_g=4.8$ V shows this difference especially well, and the two examples at $V_g=1.25$ and 1.6 V show how the potential drops along the thin and thick regions switch character as the quantized region switches from the thin to the thick region. This general character would not be expected in the infinite-connection model, where this potential drop would reflect only the characteristics of the region they are probing. For this model, as with a noninteracting one, we would expect the potential drop along one side to only give the quantum oscillations of the region they are directly probing.

The infinite-connection model would also predict a lower value of the potential drop along the nonquantized side of the sample at $V_g=4.8$ V than at 1.6 V due to the smaller value of ρ_{xx} in between the higher Landau levels. Again, the infinite-connection model does not correlate well with the observed data.

The interactive-boundary model predicts exactly what is observed. As noted in the Appendix, the magnitude of the V_{xx} potential drop along the nonquantized region depends on the ratio of ρ_{xy} of the quantized region to the effective value of R_{SD} of the nonquantized region (as if it were not contiguous with any other regions). Smaller values of R_{SD} of the nonquantized region would result in a larger V_{xx} potential drop measured along the side of the nonquantized region. At 4.8 V in Fig. 3 the ratio of R_{SD} for the nonquantized region to ρ_{xy} of the quantized region should be much smaller than at 1.6 V. This would give a larger potential drop at 4.8 V than at 1.6 V, and agrees with the data. For this case, both values of R_{SD} (1.6 and 4.8 V) of the nonquantized region are probably larger than the value of ρ_{xy} for the quantized region, and the value the source-drain resistance for the whole device should be equal to the quantized-region resistance. Again, as seen in Fig. 3, this is essentially what is observed.

The results at lower fields also support the interactive-boundary model. Figure 10 shows the Hall resistance as a function of gate voltage for one of these parallel region devices at a magnetic field of 8 T and at a temperature of 1.2 K. At $V_g=1.7$ V the thin oxide region has filled the $i=8$ Landau level, and the Hall step is seen at the correct resistance value. At $V_g=2.2$ V the thick region has filled the $i=8$ Landau level, and a change in slope of the resistance is seen, but it is at a lower value than the $i=8$ Hall step. This indicates that the Hall voltage is a strong function of position along the channel when the thick region is quantized. The low value of this latter $i=8$ Hall resistance is due to the low value of ρ_{xy} and ρ_{xx} of the thin region, and is predicted by the interactive-boundary model.

To summarize the results from the contiguous regions,

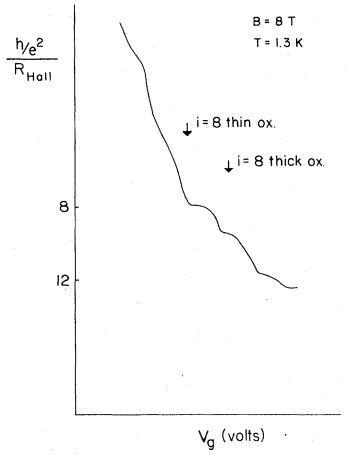

FIG. 10. Hall resistance versus gate voltage for a parallel-region device at a magnetic field of 8 T. The Hall step occurs at the correct value when the thin region is quantized, but not when the thick region is quantized.

the model where the boundary is represented by an infinite number of connections between isolated regions is clearly inadequate. The model where the interaction between the regions is determined primarily by the relative values of ρ_{xy} of the two regions does a very good job at correctly predicting the data. This model allows current to pass through the boundary between the regions, and shows that the boundary of a quantized region is not necessarily an equipotential. The success of this model allows the equipotential distribution in the quantum Hall regime to be predicted for a sample whose density varies with position in the sample, giving equipotential distributions similar to those shown in Fig. 13. In the quantum Hall regime, the current path stays in the region of minimum ρ_{xx} for a sample with inhomogeneities. The results from the analysis of these contiguous regions also predict the ability to make parallel "sandwich" devices whose Hall resistances are calculable rational fractions of the quantum Hall resistance. These fractional Hall resistances from contiguous regions are predicted to be constant with the same precision as the integer Hall resistances, currently about 0.01 ppm.

III. DISCUSSION OF "TWO-TERMINAL" QUANTIZED RESISTANCE

As a result of the success of the interactive-boundary ρ_{xy} model, we can attempt to explain the anomaly of the "two-terminal" quantized resistance. The anomaly lies in the fact that one observes the source-drain resistance to be equal to the quantized Hall resistance to within several parts in 10^5. The usual picture of the QHE in a Hall-bar sample has the current entering and leaving at the corners of the quantized region, where there is a high local electric field, into the contacts. Using appropriate values for the resistivity of doped n^+ contacts, a simple spreading resistance calculation will show that one needs the current to enter the contacts from the two-dimensional (2D) region over a space of about 10 to 100 μm in order to explain the data. This is clearly no longer possible if the current leaves at the corners of the devices. The key to explaining this comes from the interactive-boundary model, where the boundary of the 2D quantized region is not necessarily an equipotential. The region outside the boundary of the 2D quantized region will probably make some smooth transition to three-dimensional (3D) behavior. If the immediate area of the 3D contact outside the quantized 2D area has a certain effective 2D value of ρ_{xx} and (low) mobility, then in a magnetic field the region will be characterized by $\rho_{xy}=\rho_{xx}\mu H$ as well. The results from the contiguous-region experiments show that the equipotentials (and thus the current) can cross the boundary between regions in relative proportion to the ratio of the two values of ρ_{xy} of the regions. For certain contacts, this will allow the current to enter the contact area from the 2D quantized region over a broad length, giving a two-terminal resistance close to the quantized Hall resistance.

It is interesting to note that the two-terminal quantized resistance would not exist for samples with very-low-resistivity contacts corresponding to high doping levels. Such samples would be characterized by a very small value of ρ_{xy} in the contact just outside the quantized region, and most of the current would leave at the corners of the samples. This would give a large series resistance due to the spreading resistance of the contact, resulting in a two-terminal resistance quite different from the quantized resistance. This is observed in samples we have made where the doping of the n^+ contact was very high. These samples give a two-terminal resistance which is several hundred ohms larger than the quantized resistance. In addition, this series resistance should be larger at the lower-Landau-level indices due to the larger mismatch in ρ_{xy} values, and has been observed.

APPENDIX: MODELS FOR CONTIGUOUS REGIONS

1. Multiple-connection model

This model is an extension of the multiple-connection scheme for isolated regions.[4,5] The two regions are represented as isolated regions with an infinite number of connections along one edge that represents the common boundary of the regions. This model is presented for the case of closed-geometry devices (e.g., Hall bars) as this is the more illustrative case, with open geometries (e.g., Corbino disks) giving little in the way of observable predictions. The model relies on the discontinuity in potential at any point on the perimeter where current enters or leaves the region to determine the equipotential distribution at the boundary. The potential difference across any entering or leaving current element is equal to $I\rho_{xy}$ regardless of whether the region characterized by ρ_{xy} is quantized or nonquantized.[6] Multiple connections of quantized regions therefore reduce to simple comparisons of potentials on the perimeter, and are easily calculated. These results can be easily extended to any case involving nonquantized regions. For all cases, the boundary is represented as a collection of n interconnections as shown in Fig. 11.

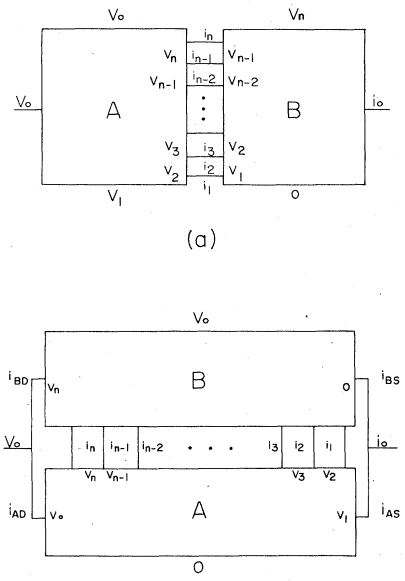

FIG. 11. The representation of the boundary between regions as given in the multiple-connection model.

a. Two quantized regions

(i) Series regions. The current i_j in the jth interconnection relative to the total current i_0 through the configuration is

$$i_j = i_0 \frac{f^{j-1}(1-f)}{1-f^n} ,$$

the voltage V_j following the jth interconnection relative to the S-D voltage V_0 is

$$V_j = (V_0 - f i_0 R_B)(1+f+f^2+\cdots+f^{j-1}) ,$$

and the value of R_{SD} is

$$R_{SD} = R_B \left[\frac{1-f}{1-f^n} + f \right] ,$$

where R_A is the quantized resistance for region A, and in all the above equations f is the ratio of the Landau-level index associated with region A to the Landau-level index associated with region B.

For any differing contiguous regions this model would predict the following: (a) the current at the boundary would all pass through a very narrow channel (becoming a point as the current tends to zero) at one side of the sample; (b) the S-D resistance of the configuration would be the quantized resistance of the lower-Landau-level-index region; and (c) the Hall resistance for each region would be the quantized resistance expected for that region. These results are shown pictorially in Fig. 12.

(ii) Parallel regions. The current i_j in the jth interconnection relative to the total current i_0 through the configuration is

$$i_j = i_0 \frac{f^j}{1+f+f^2+\cdots+f^{n+1}} ,$$

voltage V_j following the jth interconnection relative to the S-D voltage V_0 is

$$V_j = V_0 \frac{1+f+\cdots+f^j}{1+f+f^2+\cdots+f^n} ,$$

and the Hall resistance as well as R_{SD} is

$$R_{SD} = R_A \frac{1+f+\cdots+f^n}{1+f+f^2+\cdots+f^{n+1}} ,$$

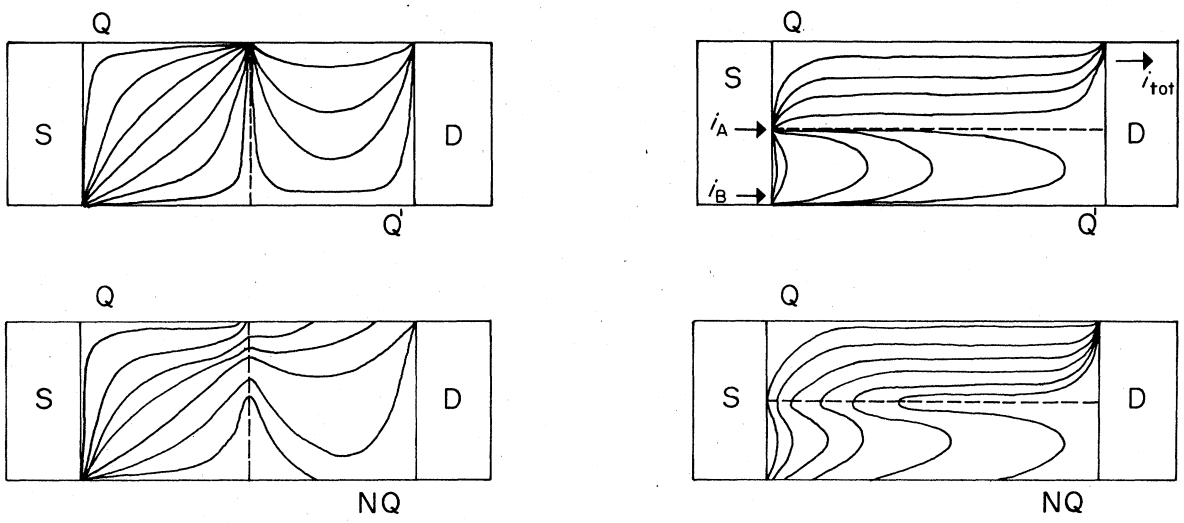

FIG. 12. Approximate equipotential distributions as given by the multiple-connection model. Series and parallel regions are shown for both cases Q-Q (both regions quantized) and Q-NQ (one region quantized, one nonquantized).

where f is the ratio of the Landau-level indices of regions A and B.

For any differing contiguous regions this model would predict the following: (a) some current enters into the higher-Landau-index region directly from the source [the amount is equal to $V_0/\rho_{xy}(A)-V_0/\rho_{xy}(B)$]; (b) the current in the lower-index region is all directed into the higher-index region within a small region at the boundary near one of the end contacts; and (c) the Hall resistance and R_{SD} are equal to the quantized resistance of the higher-index region. These results are shown pictorially in Fig. 12.

It is worth noting at this point that this model makes an odd prediction for the case of $f=1$ (same quantized region in both halves of the device). In this case the current in each interconnection is predicted to be equal to $i_n=i_0/n$. This says the current would be uniformly distributed perpendicular to the sides of the device (for this parallel case), while we know it will be parallel to the sides for a long device. Furthermore, it sets up a linear potential profile along the boundary from the source to the drain, which is also contrary to the expected results. These problems are inherent to this model since we are trying to represent an internal phenomenon by creating artificial boundaries.

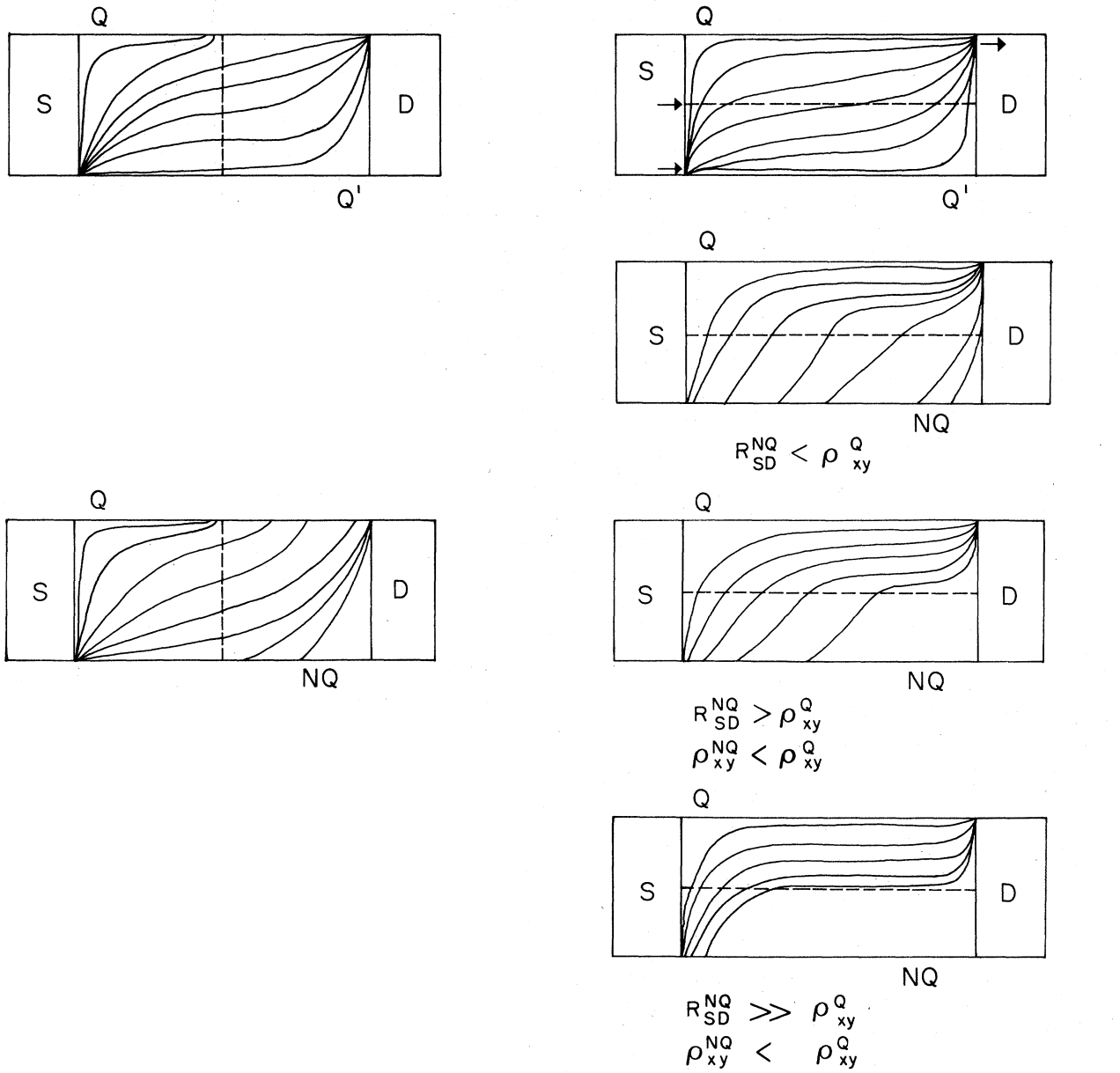

FIG. 13. Approximate equipotential distributions as given by the interactive-boundary model for both series and parallel cases. For parallel regions in the Q-NQ case (one region quantized, one nonquantized) the distribution also depends on the value of ρ_{xx} of the nonquantized region as shown through the effective value of the source-drain resistance of the nonquantized region.

b. A quantized and a nonquantized region

The extension of this model to a quantized and a nonquantized region is fairly simple. We will look at the case where the number of interconnections n is very large, which probably best represents the contiguous boundary. In the previous case of two quantized regions, the current was found to be directed between regions within a small region near the end (parallel case) or side (series case) of the sample. It is important to determine how a contiguous nonquantized region affects this result. The resistive drop between interconnections is very small compared to the discontinuity in potential due to the difference in ρ_{xy} between the regions. This is easily shown to be the case by noting that the resistive drop between current elements is $\rho_{xx}(x/w)$, where x/w becomes very small as the number of connections increases, while the potential discontinuity is not a function of the distance between current elements. So the current is still directed between regions within a very small region at the boundary. Only in the case of equal values of ρ_{xy} for the two regions will the current in these connections become small, and this is not the case of interest.

For series regions we still have the correct quantized Hall resistance in the quantized region and a similar current distribution at the boundary. For parallel regions we have a similar current distribution at the boundary, but the Hall resistance is equal to the resistance of the quantized region only if it is less than the value of ρ_{xy} of the nonquantized region. This last point can be seen by noting that the solution of the isolated multiple connected regions is dominated by the region with the lower value of ρ_{xy}. The approximate equipotential distributions for both parallel and series regions are shown in Fig. 12 for a particular polarity of magnetic field.

2. Interactive-boundary ρ_{xy} model

a. Two quantized regions

In this model equipotential lines and therefore current lines are allowed to cross the boundary between regions anywhere along its length. The interaction between regions is determined primarily by the relative values of ρ_{xy} of the contiguous regions. The model is again presented for closed geometries (e.g., Hall bars) for comparison. The case of open geometries (e.g., Corbino disks) is a trivial extension of the properties of the closed-geometry case.

(i) Series regions. In this model there is a potential discontinuity across the boundary between series regions which is equal to $I(\rho_{xy}^{A}-\rho_{xy}^{B})$, where I is the current through the entire device and the superscripts A and B refer to the two contiguous regions. The "interactive" boundary allows current and equipotential lines to cross the boundary between regions, but some of the current is forced to pass through a small region on one side of the boundary. The current that passes through this narrow region is then equal to $I(1-\rho_{xy}^{A}/\rho_{xy}^{B})$. The rest of the current is free to pass through the boundary. This situation is shown in the equipotential distribution depicted in Fig. 13. Each region is still characterized by its respective quantized Hall resistance.

(ii) Parallel regions. The behavior for this situation is complementary to that of the series regions. Each region of the series configuration has the same current passing through it, with a resultant potential discontinuity across the boundary on one side of the device. Here both regions have the same voltage across them (source to drain) with a current discontinuity across the boundary on one end of the device. These properties are basically due to the fact that the current-voltage relationship in each region must correlate with the quantized resistance for that region. The equipotential distribution for this case is also shown in Fig. 13. This distribution looks very similar to that expected for a single quantized region since both regions are quantized. The only difference is that here current is injected into the sample at the boundary between regions on one end as well as at the corners of the device. The Hall voltage is just the Hall voltage expected of the region with the lower-Landau-level index.

It should be noted that current enters the sample at the boundary between regions *without* any accompanying local high electric field just inside the 2D region. This is an unexpected result and raises questions about the current distribution in a single quantized region, since this situation allows current to enter the quantized region with almost no resistive loss at the 2D contact boundary.

b. A quantized and a nonquantized region

(i) Series regions. This situation requires virtually no alteration from the results for two quantized regions. The potential discontinuity across the boundary is always equal to the difference between the ρ_{xy} values of the respective regions, whether quantized or nonquantized. That part of the current which is constrained to pass through a small region near one side of the sample is calculated the same way as with two quantized regions. The equipotential distribution for the case of a quantized region contiguous with a nonquantized region is shown in Fig. 13.

(ii) Parallel regions. The equipotential and current distributions for this case are determined by the relative values of the source-drain resistance as calculated separately for each region. For the quantized region this is just ρ_{xy}. For a nonquantized region R_{SD} is a function of both ρ_{xy} and ρ_{xx}, which can be approximated as

$$R_{SD}=\rho_{xy}+\rho_{xx}l/w\ .$$

This is a very good approximation for long samples and not too far off for wide samples. The situation for these parallel regions now divides naturally into two separate cases: (1) ρ_{xy} of the quantized region is less than R_{SD} of the nonquantized region, and (2) ρ_{xy} of the quantized region is greater than R_{SD} of the nonquantized region.

In case (1) no current enters the device at the

boundary between regions, and all the current from the nonquantized region crosses the boundary into the quantized region. The distance over which all the current enters the quantized region and beyond which there are no more equipotentials intersecting the side of the nonquantized region is determined by the size of R_{SD} of the nonquantized region. The situation represented by this case is shown in Fig. 13 for two values of R_{SD} of the nonquantized region.

In case (2) some current enters the device at the boundary between regions, with the amount depending on the difference between R_{SD} for the nonquantized region and ρ_{xy} for the quantized region. In this case there are equipotentials throughout the nonquantized region, as shown in Fig. 13.

---

*Currently at the National Magnet Laboratory, Cambridge, Massachusetts 02139.

[1]K. von Klitzing, G. Dorda, and M. Pepper, Phys. Rev. Lett. **45**, 494 (1980).

[2]D. C. Tsui, H. L. Stormer, and A. C. Gossard, Phys. Rev. Lett. **48**, 1559 (1982).

[3]F. F. Fang and P. J. Stiles, Phys. Rev. B **27**, 6487 (1983).

[4]F. F. Fang and P. J. Stiles, Phys. Rev. B **29**, 3749 (1984).

[5]D. A. Syphers, F. F. Fang, and P. J. Stiles, Sur. Sci. **142**, 208 (1984).

[6]D. A. Syphers, Ph.D. thesis, Brown University, 1985.